Theory for the Hydrodynamic and Electrophoretic Stretch of Tethered B-DNA

Dirk Stigter* and Carlos Bustamante#
*Institute of Molecular Biology and #Howard Hughes Medical Institute, Institute of Molecular Biology and Department of Chemistry, University of Oregon, Eugene, Oregon 97403 USA

ABSTRACT We have developed a theory for the extension and force of B-DNA tethered at a fixed point in a uniform hydrodynamic flow or in a uniform applied electric field. The chain tethered in an electric field is considered to be subject to free electrophoresis compensated by free sedimentation in the opposite direction. This allows the use of results of free electrophoresis for including the effects of small ions. The force on the chain is derived for a sequence of ellipsoidal segments, each twice the persistence length of the wormlike chain. Hydrodynamic interaction between these segments is based on the long-range limit of flow around the prolate ellipsoids, as derived from equivalent Stokes spheres. The chain extension is derived by applying the entropic elasticity relation of Marko and Siggia (1995 *Macromolecules*. 28:8759–8770) to each segment for polymer chains under constant tension. We justify this procedure by comparing with extension results based on the Boltzmann averaged orientation of straight, freely jointed segments. Predicted results agree well with recent extension-flow experiments by Perkins et al., 1995. *Science*. 258:83–87, and with electrophoretic stretch experiments by Smith and Bendich (1990 *Biopolymers*. 29:1167–1173) on fluorescently stained B-DNA. We find that the equivalence of hydrodynamic and electrophoretic stretch, proposed by Long et al. (1996 Phys. Rev. Lett. 76:3858–3861; 1996 Biopolymers 39:755–759), is valid only for very small chain deformations, but not in general.

INTRODUCTION

Micromanipulation of single molecules has added considerably to our knowledge of B-DNA (Smith et al., 1992, 1996; Wang et al., 1997). This paper presents a theory for the stretching of single, tethered B-DNA molecules (1) in a uniform liquid flow (hydrodynamic stretch), and in comparison with experiments by Perkins et al. (1995), and (2) in a uniform external electric field (electrophoretic stretch) and comparison with experiments by Smith and Bendich (1990).

Our treatment is based on the wormlike chain model of Kratky and Porod (Doi and Edwards, 1986). We also consider the freely jointed chain (Flory, 1953). Bustamante et al. (1994) and Marko and Siggia (1995) have shown that the entropic elasticity of B-DNA under constant tension is described considerably better by the wormlike chain than by the freely jointed chain model. Their work confirmed earlier Monte Carlo results by Vologodskii (1994). In the experiments under study the tension in the chain increases from zero at the free end to a maximum tension at the tethered end of the chain. We expect that also in this case of stretching B-DNA under variable tension the wormlike chain is superior to the freely jointed chain. Although our predicted extensions are for the wormlike model, we use the freely jointed chain model to estimate effects of fluctuations on the chain extension.

Marko and Siggia (1995) have treated the hydrodynamic stretch of the wormlike chain on the basis of an average tension and an overall coil deformation. By using an adjustable parameter they could match experimental chain extensions to within a few percent. Larson et al. (1997) have treated hydrodynamic stretch of DNA by distributing the friction force onto a sequence of 40 or 80 beads connected together with short submolecules whose elasticity is described by the approximate Marko-Siggia relation (Bustamante et al., 1994). The friction on the chain is fitted to the known extreme values: that is, the experimental value of coiled DNA, and the theoretical value of fully stretched, rodlike DNA with 1 nm radius. Predictions of this theory are in good agreement with experiments. In a more detailed theory, also without adjustable parameters, B. H. Zimm (1997, personal communication) has treated the hydrodynamic stretch problem in a similar way. He divides the chain in sections of one persistence length each, over which the tension is assumed constant. This allows the use of an accurate inverse Marko-Siggia relation to obtain the extension of each section. Friction forces on the chain sections are evaluated with standard methods in polymer hydrodynamics, adapted to a bead model with wormlike chain statistics.

Electrophoretic stretch of B-DNA has been treated by Schurr and Smith (1990) for the freely jointed chain, and by Marko and Siggia (1995) for the wormlike chain. In both cases the electric force on the small ions was neglected, and the charge density of B-DNA was used as an adjustable parameter. Long et al. (1996a,b) have predicted extension in electric fields by using the experimental data on hydrody-

Received for publication 5 December 1997 and in final form 11 May 1998.
Address reprint requests to Dr. Dirk Stigter, 1925 Marin Ave., Berkeley, CA 94707. Tel.: 510-526-4989; E-mail: stigter@maxwell.ucsf.edu.
This work was presented in part at the International Interdisciplinary Workshop on Structure and Function of DNA: A Physical Approach, Abbaye du Mont Sainte-Odile, Alsace, France, September 29–October 5, 1996.

0006-3495/98/09/1197/14 $2.00

namic stretch by Perkins et al. (1995). It is our aim to develop a theory without adjustable parameters by using the structural charge density of B-DNA.

The theory in the present paper has three interconnected parts: the hydrodynamic force on the chain. the electrophoretic force on the chain, and the resulting chain extension. Both forces and the relative extension vary along the tethered chain. Below we indicate the approach to each part of the theory.

The hydrodynamics of the wormlike chain were treated for diffusion and intrinsic viscosity by Yamakawa and Fujii (1973, 1974), using the Oseen-Burgers procedure for slender body hydrodynamics. We have not tried to extend their approach to the problem under study because we prefer to use the same chain model for both the electrophoretic and the hydrodynamic force. For hydrodynamic purposes we model the chain as a sequence of straight segments and represent each segment by a prolate ellipsoid, using friction coefficients derived from Oberbeck's work (1876). Interactions between segments are treated with methods familiar in polymer theory (Kirkwood and Riseman, 1948; Garcia de la Torre and Bloomfield, 1977), but we keep track of segment orientation by using unaveraged, directional flow perturbations from each segment.

Electrophoretic stretch is closely connected to free electrophoresis. Modifying the theory of Schurr and Smith (1990) or of Marko and Siggia (1995) by introducing the electric force on the small ions near DNA may seem a complicating factor. No explicit treatment of this extra electric force, however, is required here, because the results can be transferred directly from the theory of free electrophoresis (Stigter, 1991). The latter theory is available for charged rods (Stigter, 1978a,b), but not for curved cylinders or other models of the wormlike chain. Therefore, we straighten short sections of the wormlike chain as above. The choice of the length of the straight segments is based on the statistics of the wormlike chain as follows.

Let α denote the angle between the tangents to the chain at point Q and a second point separated by contour length s. Then the flexibility of the chain is given by its persistence length P in the expression for the average of cos α (Landau and Lifshitz, 1958)

$$\langle \cos \alpha \rangle = \exp(-s/P) \tag{1}$$

This expression gives the decaying correlation between the chain directions for growing distance s along the chain between the two points. For $s \gg P$ there is no correlation, $\langle \cos \alpha \rangle \to 0$. For $s \ll P$ the correlation is maximal, $\langle \cos \alpha \rangle \to 1$. We approximate the exponential decay of $\langle \cos \alpha \rangle$ by choosing $\langle \cos \alpha \rangle = 1$ for $s < P$ and $\langle \cos \alpha \rangle = 0$ for $s > P$. Since the memory loss of the chain orientation decays according to Eq. 1 on both sides of a given point Q in the chain, the straight section, with $\langle \cos \alpha \rangle = 1$, has a length $2P$, and has no orientational correlation, $\langle \cos \alpha \rangle = 0$, with the adjacent straight sections, also of length $2P$. It is well known that this approximation of the wormlike chain, usually called the freely jointed chain, gives for long chains the same mean square end-to-end distance. It is reasonable to derive the hydrodynamic and electrophoretic forces on the wormlike chain from the same approximation.

The relation between stretching forces and chain extension has been treated in two ways. First, Schurr and Smith (1990) have treated electrophoretic stretch for the freely jointed chain by converting the stretching force on each segment into a potential energy. Then this energy was used in the Boltzmann statistics of each segment to find its average orientation and, hence, its average contribution to the extension of the chain. Second, Marko and Siggia (1995) dealt with electrophoretic stretch, and Larson et al. (1997) and Zimm (1997, personal communication) with hydrodynamic stretch in a more direct way. They derived the stretching force on short sections of the wormlike chain, and applied the Marko-Siggia results for the entropic elasticity under constant tension to each section separately to find the total chain extension. The Marko-Siggia force-extension treatment is for long chains. The above application to short chain sections may compromise the wormlike nature of the chain, or may treat fluctuations incorrectly. To estimate possible errors we compare the Boltzmann method and the direct force-extension method for the freely jointed chain.

For the main calculations we use the straight segment approximation to obtain the stretching forces, and to find the total chain extension we apply Zimm's (1997, personal communication) inverse Marko-Siggia force-extension relation to the single segments. The computation of chain conformation and tension along the chain is iterated until self-consistent results are obtained. We start with hydrodynamic stretch, then proceed with the more involved case of electrophoretic stretch. In the application to gel electrophoresis, stretching forces are at least as important as chain extensions. Therefore, we give results for both the chain extension and for the tethering force versus the strength of the external field. We also compare hydrodynamic and electrophoretic stretch to test an idea proposed by Long et al. (1996a) of "a hydrodynamic equivalence that, in particular, predicts that an end-anchored polyelectrolyte deforms in a similar way in an electric field E_∞, and in a hydrodynamic flow at velocity $v_\infty = \mu_{el} E_\infty$ (where μ_{el} is the electrophoretic mobility of the polyelectrolyte)."

In an earlier version of this paper we applied the Schurr-Smith (1990) statistics to treat hydrodynamic stretch. This work was criticized because, according to a reviewer, the use of a friction related-energy in a Boltzmann factor is unacceptable. The use of friction forces in statistical mechanics has, however, a firm foundation in early polymer hydrodynamics (Kramers, 1946; Hermans, 1949). In a classic paper (1946) Kramers explained that if the effect of friction forces is the same as that of a potential energy, this energy may be used in Boltzmann statistics. We show that such is the case in our treatment (see Eq. 19 below). A somewhat different argument is that, for a polymer that is

stationary in a flow field, the field of friction forces balances a force field derived from the deformation potential of the polymer which is part of its free energy and, therefore, may be used in statistical mechanics of the polymer.

TENSION IN A CHAIN TETHERED IN UNIFORM FLOW

We model the chain as a sequence of N freely rotating straight segments, each of length $2P$, which is twice the persistence length of the chain. The chain is tethered at segment 1 in a uniform flow with velocity u in the positive z direction of the Cartesian coordinates. Segments 1, . . . i, . . . N make angles θ_1, . . . θ_i, . . . θ_N with the positive z axis, see Fig. 1.

We are interested in the components of forces and liquid velocities along the z axis. Let u_i be the z component of the liquid velocity at segment i. When segment i makes an angle θ_i with the z axis (see Fig. 2), the component of u_i parallel with the segment is

$$u_{\parallel} = u_i \cos\theta_i \tag{2a}$$

and the component perpendicular to the segment

$$u_{\perp} = u_i \sin\theta_i \tag{2b}$$

When $f_{\parallel}$ and $f_{\perp}$ are the friction coefficients of the segment for orientation parallel and perpendicular to the flow direction, respectively, the liquid velocity u_i subjects the segment to the forces

$$F_{\parallel} = u_{\parallel} f_{\parallel} \tag{3}$$

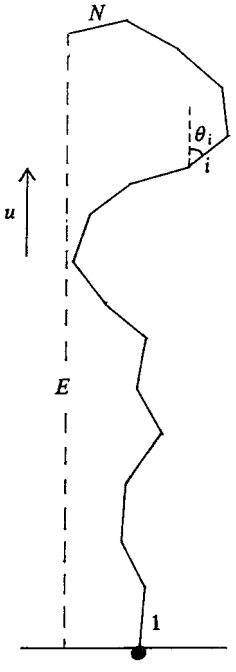

FIGURE 1 Freely jointed chain of N segments, tethered at segment 1 in liquid with velocity u along z axis, with extension E in flow direction.

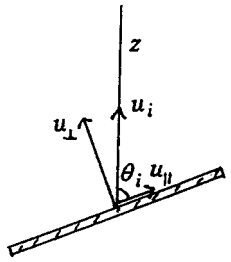

FIGURE 2 Component u_i in z direction of liquid velocity at segment i and its components parallel and perpendicular to segment.

and

$$F_{\perp} = u_{\perp} f_{\perp} \tag{4}$$

We assume that the total friction force on a segment is exerted on its center. The z component of this force, F_i, is the sum of the z components of $F_{\parallel}$ and $F_{\perp}$ (see Fig. 3).

$$F_i = F_{\parallel}\cos\theta_i + F_{\perp}\sin\theta_i = u_i(f_{\parallel}\cos^2\theta_i + f_{\perp}\sin^2\theta_i) \tag{5}$$

For the purpose of hydrodynamics each chain segment is modeled as a prolate ellipsoid with long axis $2P$ and short axes c. Following results by Happel and Brenner (1965) based on Oberbeck's treatment (1876), the friction coefficient for flow parallel to the long axis is, in terms of the axial ratio $\phi = 2P/c$,

$$f_{\parallel} = \frac{4\pi\eta c}{\left[-\dfrac{\phi}{\phi^2-1} + \dfrac{2\phi^2-1}{(\phi^2-1)^{3/2}}\ln(\phi + \sqrt{\phi^2-1})\right]} \tag{6}$$

where η is the viscosity of the liquid. The friction coefficient for flow perpendicular to the long axis is

$$f_{\perp} = \frac{8\pi\eta c}{\left[\dfrac{\phi}{\phi^2-1} + \dfrac{2\phi^2-3}{(\phi^2-1)^{3/2}}\ln(\phi + \sqrt{\phi^2-1})\right]} \tag{7}$$

Equations 6 and 7 have been derived for uncharged ellipsoids. Strictly speaking, in applications to B-DNA one should make a correction for the DNA charge, that is, for

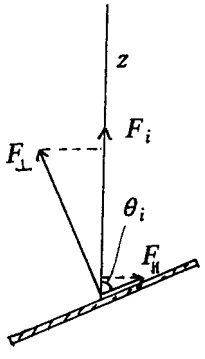

FIGURE 3 Friction forces parallel and perpendicular to segment i with vector sum F_i in z direction.

the extra force to move the counterions that is transmitted to the moving DNA. Stigter (1982) has treated this effect on the sideways motion of long charged cylinders. The charge effect on the friction coefficient of DNA is found to be around a few percent. In this paper we neglect this minor correction.

We now consider the local liquid velocity at segment i. When a chain is placed in a liquid with uniform velocity u, the presence of the stationary (tethered) chain perturbs the liquid velocity. The velocity u_i is the z component of the local liquid velocity at the center of segment i when segment i has been removed from the chain. The velocity u_i is calculated as the sum of the unperturbed velocity u and the perturbations by all other segments

$$u_i = u + \sum_{j=1}^{N} \Delta u_{ij} \quad j \neq i \tag{8}$$

Δu_{ij} is the z component of the perturbation by segment j, in its local velocity u_j, at the center of segment i (see Fig. 4). The perturbation Δu_{ij} depends on the length and direction of the distance vector between segments i and j (r_{ij} and θ_{ij} in Fig. 4), on the orientation and friction coefficient of segment j, and on the local velocity u_j. Since each evaluation of the velocity profile requires the computation of $N(N-1)$ different values of Δu_{ij}, using the exact flow pattern around an ellipsoidal segment j is too computer intensive. Therefore, we use the long-range approximation of this flow pattern, which is derived by replacing the ellipsoidal segment j by a sphere with the same Stokes friction; that is, a sphere with radius a_j given by

$$6\pi\eta a_j = f_\parallel \cos^2\theta_j + f_\perp \sin^2\theta_j \tag{9}$$

with $f_\parallel$ and $f_\perp$ from Eqs. 6 and 7. The Stokes flow around this equivalent sphere (Landau and Lifshitz, 1982) yields

$$\Delta u_{ij} = u_j\left(-\frac{3}{4}\frac{a_j}{r_{ij}} - \frac{1}{4}\frac{a_j^3}{r_{ij}^3}\right) + u_j\cos^2\theta_{ij}\left(-\frac{3}{4}\frac{a_j}{r_{ij}} + \frac{3}{4}\frac{a_j^3}{r_{ij}^3}\right) \tag{10}$$

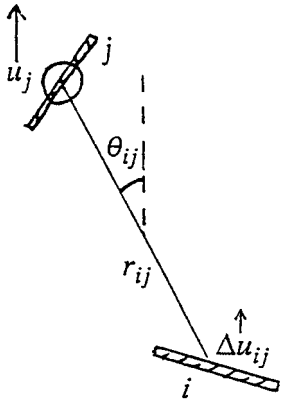

FIGURE 4 Distance r_{ij} and angle θ_{ij} for hydrodynamic interaction Δu_{ij} between segments j and i given by Eq. 10.

The distances r_{ij} and the angles θ_{ij} in Eq. 10 require the chain conformation. The change of the coordinates between segments i and $i+1$, Δx_i, Δy_i, Δz_i, is illustrated in Fig. 5. The iterative calculation described in the next section gives $\cos\theta_i$ for all i. The set of angles ϕ_i for $i = 1$ to N is chosen randomly between 0 and 2π. The coordinates of the segments are determined by accumulation: $x_i = \Sigma_{j=1}^{i} \Delta x_j$, etc. The distances r_{ij} are obtained with

$$r_{ij} = [(x_i - x_j)^2 + (y_i - y_j)^2 + (z_i - z_j)^2]^{1/2} \tag{11}$$

and the angles θ_{ij} with

$$\cos\theta_{ij} = \frac{z_i - z_j}{r_{ij}} \tag{12}$$

The tension at segment i, T_i, equals the friction on the loose end of the chain, downstream from segment i. We neglect in T_i the friction on segment i itself, and also any tension variation over each segment i, which are good approximations for large N. Furthermore, in evaluating the tension on segment i, we assume that the rest of the chain is frozen in its average conformation. Thus we have with Eq. 5

$$T_i = \sum_{k=i+1}^{N} F_k = \sum_{k=i+1}^{N} u_k(f_\parallel\langle\cos^2\theta_k\rangle + f_\perp\langle\sin^2\theta_k\rangle) \tag{13}$$

where the angular brackets indicate segmental averages, obtained as explained in the next section. The tethering force, F_t, equals the total friction force on the chain

$$F_t = \sum_{k=1}^{N} F_k. \tag{14}$$

CHAIN EXTENSION IN HYDRODYNAMIC STRETCH

Each segment contributes on average $\Delta z_i = 2P\langle\cos\theta_i\rangle$ to the extension of the chain in the z direction, so the total

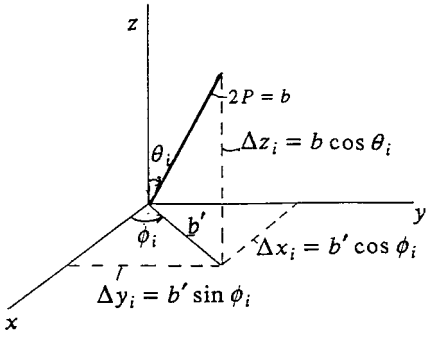

FIGURE 5 Cartesian coordinates of segment i with length $2P = b$ used to calculate chain conformation with random choice of angle ϕ_i.

extension Ex of the chain along the z axis is the sum

$$Ex = \sum_{i=1}^{N} \Delta z_i = 2P \sum_{i=1}^{N} \langle \cos \theta_i \rangle \tag{15}$$

There are several ways to connect $\langle \cos \theta_i \rangle$ with the tension T_i in segment i. Here we first apply to each segment the Marko-Siggia (1995) results for the wormlike chain under constant tension. We use an expression derived by Zimm (1997, personal communication) which is an excellent approximation of the exact results and reads in the present notation

$$\langle \cos \theta_i \rangle = \frac{0.6667 t_i + 0.8080 t_i^2 + 0.10365 t_i^3}{1 + 1.1118 t_i + 1.1076 t_i^2 + 0.10365 t_i^3} \quad t_i \leq 9$$

$$\langle \cos \theta_i \rangle = 1 - 1/(4t_i)^{1/2} \quad t_i > 9 \tag{16}$$

In Eq. 16 t_i is the dimensionless reduced tension related to the tension T_i in Eq. 13 and to the persistence length P of the wormlike chain

$$t_i = \frac{T_i P}{kT} \tag{17}$$

where k is Boltzmann's constant, and T is the absolute temperature.

Second, we relate the segmental averages in Eqs. 13 and 15 with the approximate expression

$$\langle \cos^2 \theta_i \rangle = \langle \cos \theta_i \rangle^2 \tag{18}$$

The averages in Eq. 16 can be computed sequentially for all segments $i = N, N-1, \ldots 1$, because the expression for segment i requires information only about the segments $k = i+1$ to N, toward the free end of the chain. As shown schematically in Fig. 6, the computation of the chain extension is iterative, starting, for example, from the completely stretched chain, with $\cos \theta_i = 1$ for all i. In each iteration step Eqs. 8 and 10 yield a new set of u_i values, which is then used with Eqs. 13 and 16 to find a new chain conformation, until the force F_t on the chain in Eq. 14 has become stable. We use the same random set of angles ϕ_i (see Fig. 5) in all iteration steps.

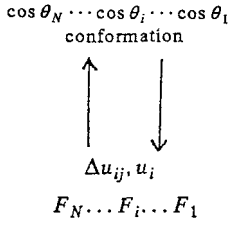

FIGURE 6 Iteration scheme.

Equations 16 and 18 require further consideration. Equation 16 has been derived for long chains (Marko and Siggia, 1995; Zimm, 1997, personal communication). The application to single chain segments might introduce significant fluctuation errors, depending on the range available to the segment orientation. For example, for very small tensions, when in Eq. 15 $Ex \to 0$, statistics yield $\langle \cos \theta_i \rangle \to 0$ and $\langle \cos^2 \theta_i \rangle \to \frac{1}{3}$. Conversely, Eq. 18 gives $\langle \cos^2 \theta_i \rangle \to 0$. We investigate this fluctuation effect for the freely jointed chain where the translational friction in the flow direction is used in the Boltzmann statistics of the segment orientation. This produces the correct statistical averages of $\cos \theta_i$ and of $\cos^2 \theta_i$ for all segments.

The derivation of $\langle \cos \theta_i \rangle$ is treated as diffusion in an external field. For flow velocity $u = 0$, θ_i is determined by free rotational diffusion. In that case all orientations of segment i have the same statistical weight; that is, all values of $\cos \theta_i$ are equally probable, and any frictional energy for segment rotation is supplied by the thermal energy. For finite flow rates we assume that again the thermal energy provides the rotational friction energy of the segment, but now the rotational diffusion is biased toward the parallel orientation, toward $\cos \theta_i = 1$. This bias is due to friction forces in the z direction on the free end of the chain, downstream from segment i. In the statistics of segment i we assume that all other segments are frozen in their average orientation. As before, this yields the average tension T_i on segment i given by Eq. 13. When segment i rotates from its standard state, $\theta = \pi/2$, to $\theta = \theta_i$, the change in segment position can be viewed as a series of small rotations around the center of the segment, each followed by a small translation in the z direction of the segment with constant orientation under the influence of the tension T_i. The energy involved in the translation is recoverable, the hallmark of a potential energy, and is given by the force integral

$$U_i = -\int_0^{2P \cos \theta_i} T_i dz = -2PT_i \cos \theta_i \tag{19}$$

Considering U_i as the potential field in which the rotational diffusion of segment i occurs, we find its Boltzmann averaged position from

$$\langle \cos \theta_i \rangle = \frac{\int_{-1}^{1} \cos \theta_i \exp(-U_i/kT) d(\cos \theta_i)}{\int_{-1}^{1} \exp(-U_i/kT) d(\cos \theta_i)} = \coth(2t_i) - \frac{1}{2t_i} \tag{20}$$

where t_i is given by Eq. 17. Equation 20 is usually derived as the entropic elasticity of long chains (Hill, 1960). It is for the freely jointed chain the equivalent of Eq. 16 for the wormlike chain. The mean square value of $\cos \theta_i$ is

$$\langle \cos^2 \theta_i \rangle = \frac{\int_{-1}^{1} \cos^2 \theta_i \exp(-U_i/kT) d(\cos \theta_i)}{\int_{-1}^{1} \exp(-U_i/kT) d(\cos \theta_i)} = 1 + \frac{1}{2t_i^2} - \frac{\coth(2t_i)}{t_i} \tag{21}$$

We can now treat the hydrodynamic stretch of freely jointed chains by using Eq. 20 instead of Eq. 16 for $\langle \cos \theta_i \rangle$. To test the effect of fluctuations we can then use approximation Eq. 18 and compare with more accurate results obtained with Eq. 21 for $\langle \cos^2 \theta_i \rangle$. Fig. 7 shows results for stained B-DNA with contour length $2NP = 21.8$ μm, assuming $P = 675$ Å for the persistence length and 24 Å for the chain diameter, as argued later. The top curve was evaluated with Eqs. 20 and 21, the middle curve with Eqs. 20 and 18, and the bottom curve with Eqs. 16 and 18. The small difference between the top and the middle curves for the freely jointed chain shows that fluctuations are not important, and that Eq. 18 is a good approximation for $\langle \cos^2 \theta_i \rangle$. The bottom curve for the wormlike chain is substantially lower than the results for the freely jointed chain, of the order of 10%. All further computations in this paper are for wormlike chains, using Eqs. 16 and 18.

We proceed with electrophoretic stretch of polyelectrolytes. Here the extension treatment is the same as given in this section for hydrodynamic stretch. Only the derivation of the tension along the chain is different.

ELECTROPHORETIC STRETCH

The tethered B-DNA is stationary in the electric field E in the z direction. We first derive the tension on each straight segment. In the theory of Schurr and Smith (1990) the tension arises from the force exerted by the field E on the charge fixed to the DNA. In a more recent paper, Stigter (1991) also considered the electric force on the surrounding ion atmosphere which is partly transmitted as an increased viscous drag of the DNA. At present we add the long-range hydrodynamic interactions between the various chain segments.

The derivation of the tension in the chain is similar to that leading to Eq. 13. With the same approximations as in Eq. 13, we have for the tension in segment i

$$T_i = \sum_{k=i+1}^{N} F_k \tag{22}$$

where now the force F_k does not relate to a flow field u, but F_k is the "electrophoretic force" on segment k in the electric field E. Explicit introduction of the role of the small ions leads to considerable complexity in the treatment of the electrophoretic force F_k. The analysis is, however, greatly simplified when we disregard the tether and connections between the segments, and add a hypothetical sedimentation force on each stationary chain segment. We first look at a single, isolated segment, labeled i.

If the free electrophoretic velocity of the segment i is ν_{el} in the z direction, the sedimentation force F_{sed} is assumed to be such that it gives the segment i the compensating velocity $\nu_{sed} = -\nu_{el}$. Then the sedimentation force on the stationary segment, ν_{sed} times the friction factor f_{sed} of the segment, compensates exactly the electrophoretic force F_i on it. This is the total force exerted on the stationary segment i by the electric field, given by

$$F_i = \nu_{el} f_{sed} \tag{23}$$

To introduce the segment orientation into Eq. 23 we decompose into components parallel and perpendicular to the segment. The parallel and perpendicular field components, $E \cos \theta_i$ and $E \sin \theta_i$, respectively, give the electro-

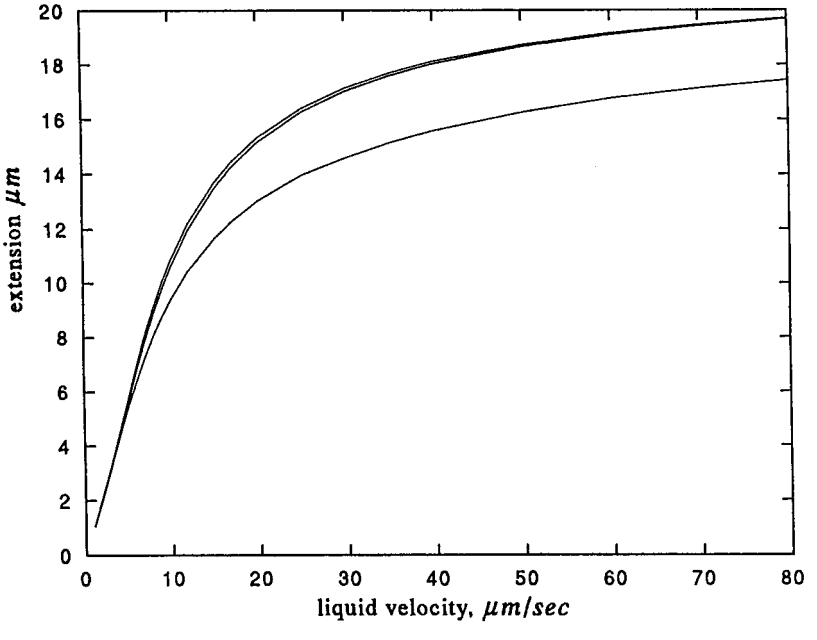

FIGURE 7 Extension-flow curves for B-DNA with contour length 21.8 μm. From top to bottom: Exact theory for freely jointed chain, Eq. 21. Approximate theory for freely jointed chain, Eq. 18. Approximate theory for wormlike chains, Eq. 18.

phoretic velocity components (Stigter, 1991)

$$\nu_{\parallel} = \frac{\epsilon_0 D\zeta E}{\eta}\cos\theta_i \tag{24}$$

$$\nu_{\perp} = \frac{\epsilon_0 D\zeta E}{\eta}\frac{2}{3}g_{\perp}\sin\theta_i \tag{25}$$

where ζ is the surface potential of B-DNA, ϵ_0 is the permittivity of free space, D is the dielectric constant of the salt solution, and $g_{\perp}$ is a numerical factor tabulated by Stigter (1991). The factor $2g_{\perp}/3$ in Eq. 25 accounts for the perturbation of the electric field by the presence of the nonconducting cylinder and by the relaxation of the ionic atmosphere around the moving cylinder. With the friction factors $f_{\parallel}$ and $f_{\perp}$ from Eqs. 6 and 7 we find for the components of F_i

$$F_{\parallel} = \nu_{\parallel} f_{\parallel} \quad F_{\perp} = \nu_{\perp} f_{\perp} \tag{26}$$

and the electrophoretic force F_i on the segment becomes

$$F_i = F_{\parallel}\cos\theta_i + F_{\perp}\sin\theta_i = \frac{\epsilon_0 D\zeta E}{\eta}\left[f_{\parallel}\cos^2\theta_i + \frac{2}{3}g_{\perp}f_{\perp}\sin^2\theta_i\right] \tag{27}$$

Equation 27 was derived for a single, isolated segment. We now consider the entire tethered chain where we need to add the hydrodynamic interactions between the segments, which become part of the electrophoretic force F_i. Such interaction depends on the liquid flow perturbation by the segments in stationary electrophoresis. We treat this as above by considering the stationary state as the sum of free electrophoresis and free sedimentation. In free electrophoresis the liquid velocity around the moving particle decays rapidly, on average proportional to the electrostatic potential in the ionic atmosphere. Alternatively, flow perturbations by sedimenting particles are long-range, as we have seen, for example, in Eq. 10.

In Fig. 8 the liquid velocity patterns around a single segment are sketched for (a) free electrophoresis, (b) free sedimentation, and for the sum (c) = (a) + (b) = stationary electrophoresis. Neglecting any contribution of the short-range free electrophoresis, we derive the intersegment interaction from the long-range free sedimentation only. We consider the forces on a segment i in the chain, The segment is subject to the electrophoretic force F_i in the z direction, and to the compensating tension forces. After eliminating the tension forces by cutting the connections with segments $i-1$ and $i+1$, we keep segment i stationary with the imaginary sedimentation force $-F_i$ on the center of the segment. All other segments are treated in the same way and now the hydrodynamic interaction is treated as before with Eqs. 9 and 10. We replace each segment by a Stokes sphere with an orientation-dependent radius such as a_j in Eq. 9 for segment j. Then the force F_j on segment j gives rise to a fluid perturbation Δu_{ij} at segment i given by the Stokes flow in Eq. 10, provided that for the local liquid velocity at

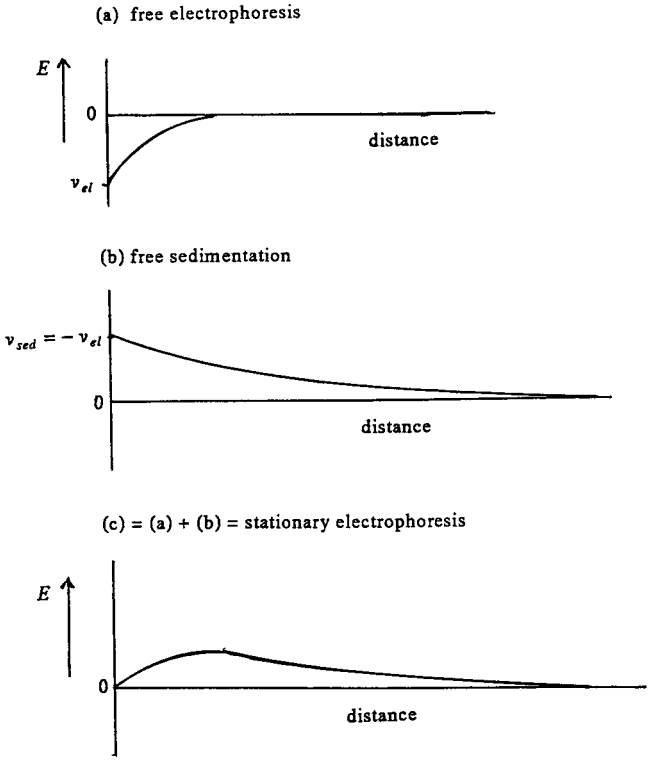

FIGURE 8 Schematic decomposition of flow around charged particle tethered in external electric field as sum of free electrophoresis and free sedimentation.

segment j we take

$$u_j = \frac{F_j}{6\pi\eta a_j} \tag{28}$$

So at segment i we find, due to the long-range hydrodynamic interaction between the segments, a liquid velocity in the z direction $\Sigma_{j=1}^{N}{}'\Delta u_{ij}$ where the prime on the summation sign indicates $j \neq i$. This liquid velocity gives on segment i the extra force $6\pi\eta a_i \Sigma_{j=1}^{N}{}'\Delta u_{ij}$. With Eq. 27 we obtain for the total electrophoretic force on segment i in the chain

$$\begin{aligned} F_i = {} & \frac{\epsilon_0 D\zeta E}{\eta}\left[f_{\parallel}\cos^2\theta_i + \frac{2}{3}g_{\perp}f_{\perp}\sin^2\theta_i\right] \\ & + 6\pi\eta a_i \sum_{j=1}^{N}{}' \frac{F_j}{6\pi\eta a_j}\left[-\frac{3}{4}\frac{a_j}{r_{ij}} - \frac{1}{4}\frac{a_j^3}{r_{ij}^3}\right. \\ & \left. + \cos^2\theta_{ij}\left(-\frac{3}{4}\frac{a_j}{r_{ij}} + \frac{3}{4}\frac{a_j^3}{r_{ij}^3}\right)\right] \end{aligned} \tag{29}$$

We note that hydrodynamic interaction always reduces the initial force on a segment, consistent with the negative sign of the second term in Eq. 29, with the opposite signs of ν_{el} in Fig. 8 *a* and the liquid velocity in Fig. 8 *c*, and with the negative sign of Δu_{ij} in Eq. 10.

With Eq. 29 we have all the elements for the computation of electrophoretic stretch. Briefly, assuming a starting con-

formation of the chain, Eqs. 29 and 22 give the tension T_i along the chain. These results are used in Eqs. 15–17 for the wormlike chain to find the chain extension and, with Eqs. 11 and 12, the chain conformation. Then, using Eq. 18, a new computation of the tension is started. In this way, similar to the iterative computation of hydrodynamic stretch, we cycle between tension and conformation until Eq. 14 indicates that the desired level of convergence has been reached.

COMPARISON OF HYDRODYNAMIC AND ELECTROPHORETIC STRETCH

We first consider chain conformations of stained B-DNA with contour length 21.8 μm, tethered in a flow field u or electric field E. The ζ potential of the DNA in units of kT/e is $\zeta e/kT = -4.65$, the electrophoretic factor in Eq. 25 is $g_\perp = 0.484$, as discussed in the next section. The values of u and E are adjusted to give the same chain extension $Ex = 11.55$ μm in both fields. The conformations are shown in Fig. 9 for a particular sequence of random choices for the angle $\phi(i)$ in Fig. 5. The stretch patterns of DNA in the two fields are distinctly different. The electrophoretic stretch is relatively higher near the tethering point, at $z = 0$, and relatively lower near the free end of the chain. This can be understood when we compare the forces on the chain.

In Fig. 10 the force per segment is plotted versus the distance z from the tethering point: solid curves for hydrodynamic stretch and dashed curves for electrophoretic stretch. The two lower curves give the full force per segment, Eqs. 5 and 8 in field u, Eq. 29 in field E. In the two upper curves the hydrodynamic interaction between segments is discounted; $\Delta u_{ij} = 0$, that is, Eq. 5 with $u_i = u$ in flow field u, Eq. 27 in electric field E. The force curves show several interesting features that are consistent with the theory.

1. The local variation of the force with z is due to the change in segment orientation, from nearly parallel to the external field near $z = 0$ to nearly random near the free end of the chain. We expect that similar force curves for the wormlike chain model would be smoother. Fig. 10 shows that even without the local fluctuations the linear force density is not constant along the chain, in particular in an electric field. So the tension does not change linearly with the distance z, as assumed by Marko and Siggia (1995) in their treatment of electrophoretic stretch;
2. The difference between the solid and the dashed curves originates in the extra factor $2/3\ g_\perp = 0.232$ in Eq. 27 in field E, which is missing in Eq. 5 for field u;
3. Fig. 10 shows that the force in field E is greater than in field u on segments near the tethered end, at $z = 0$, and smaller than in field u at the free end of the chain, the lower curves in Fig. 10 crossing around $z = 10$ μm. This is consistent with the chain conformations in Fig. 9, which are stretched more in field E near $z = 0$, and stretched less in field E near the free end of the chain. To reach the same overall chain extension, the electrophoretic stretch requires on average more force per segment than hydrodynamic stretch;
4. The difference between the upper and the lower curves in Fig. 10 shows that the intersegment interaction introduces significant fluctuations in the force per segment. This is related to the random choice of the x and y coordinates along the chain (see Fig. 5). This random choice causes considerable variation in the relative position of neighboring segments as demonstrated in Fig. 9 and, hence, in their hydrodynamic interaction.

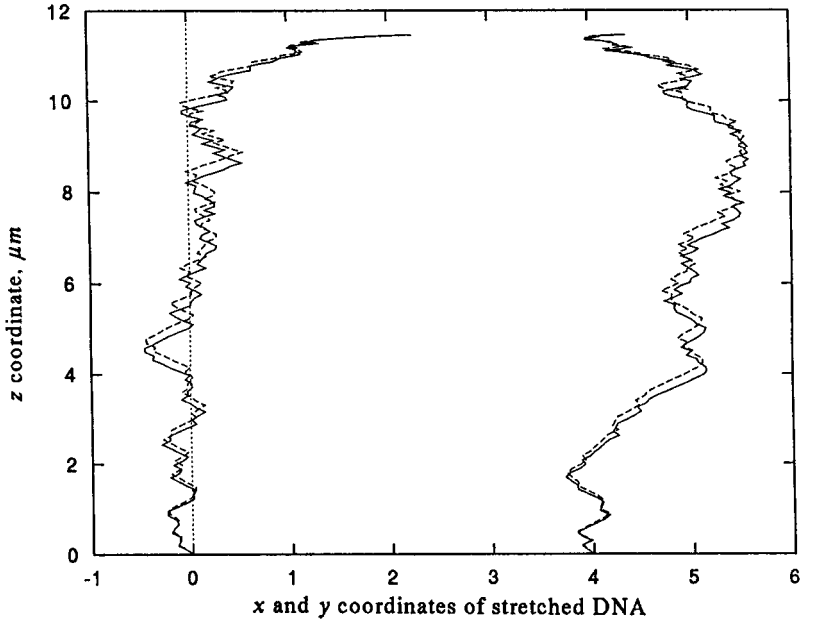

FIGURE 9 Conformation of 21.8-μm-long DNA extended to 11.55 μm in z direction by flow (*solid curves*) or electric field (*dashed curves*). x coordinates start at 0, y coordinates start at 4 μm. Note different scale of z coordinates.

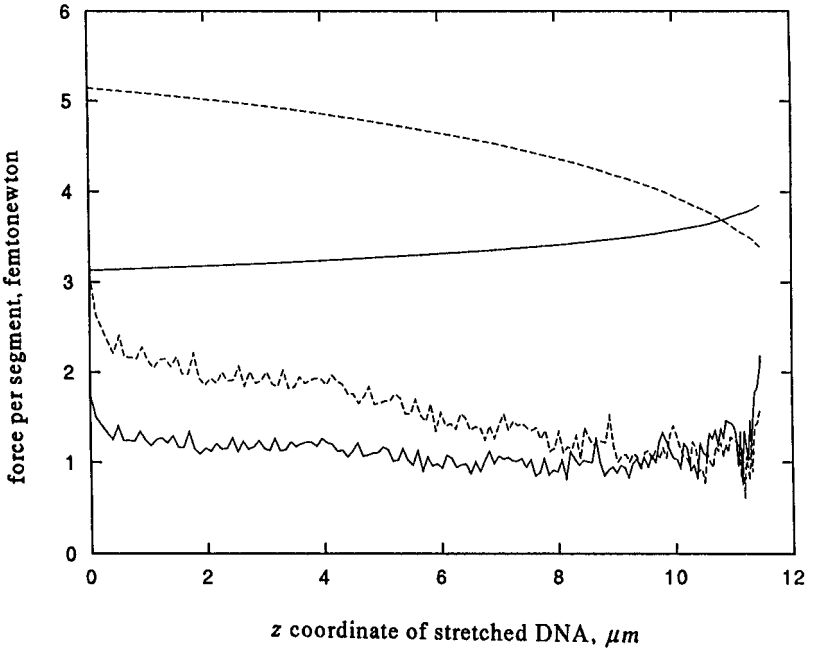

FIGURE 10 Force F_i on segment i versus coordinate z_i for DNA conformation of Fig. 9 for stretch in flow (*solid curves*) or electric field (*dashed curves*) calculated with full theory (*lower curves*) or without hydrodynamic interaction between segments (*upper curves*).

We now consider the "hydrodynamic equivalence" proposal of Long et al. (1996a,b) stating that hydrodynamic and electric fields deform a polyelectrolyte in a similar way. We evaluate the extension Ex, Eq. 15, as well as the tethering force F_t, Eq. 14, as a function of the fields u and E. Then we plot Ex versus F_t for both fields. Fig. 11 shows the results. In general, for the same force the extension is higher in a flow field than in an electric field. This agrees with the lower curves in Fig. 10. For very low extensions, however, the $Ex - F_t$ curves overlap. The reason is that for $Ex \to 0$ all segments are oriented randomly. Therefore, the $F_i - z$ curves are level and, for the same extension, will overlap, giving the same sum F_t. In summary, the equivalence of hydrodynamic and electric fields is strictly valid in the limiting case of low extensions, but not in general.

So far we have used the same set of ϕ_i values in all examples, that is, the same sequence of random numbers for the chain conformations of Fig. 9. For hydrodynamic stretch Fig. 12 gives not only the conformation of Fig. 9, but also those computed with nine other sets of random numbers, i.e., with sequences taken from different parts of the very long period of the random number generator. The ensemble of conformations in Fig. 12 looks like the experimental, time-averaged image of a tethered DNA molecule deformed

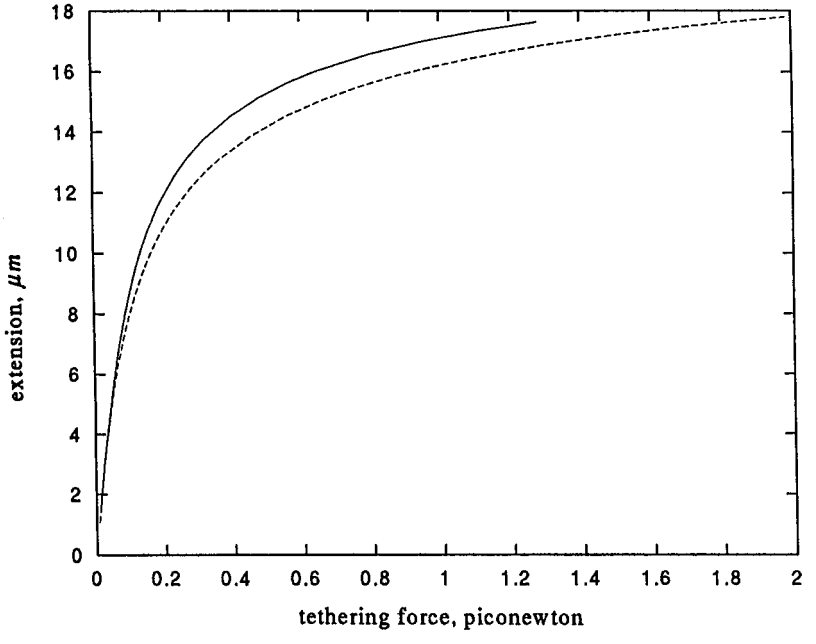

FIGURE 11 Test of hydrodynamic equivalence proposal of Long et al. (1996a,b). Extension versus tethering force curves for 21.8 μm DNA in flow (*solid curve*) or electric field (*dashed curve*).

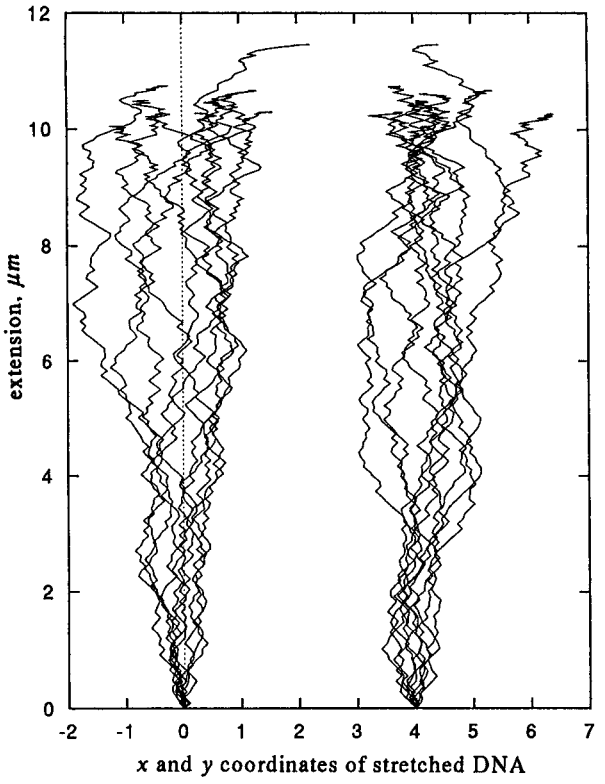

FIGURE 12 Ten different conformations of 21.8-μm-long DNA stretched in flow with velocity $u = 12$ μm/s.

by constant fluid flow (Perkins et al., 1995). Fig. 13 gives the collection of hydrodynamic stretch curves for the random sequences used in Fig. 12. The variation among the curves is significant, due to the varying contribution of the segment interactions Δu_{ij}, which are conformation-dependent. The variation among the electrophoretic stretch curves (not shown) is somewhat greater because the contributions of Δu_{ij}, measured by the difference between the upper and lower curves in Fig. 10, are larger. For longer DNA the effect of conformation on the stretch curve is relatively smaller because of more effective averaging. To dampen the influence of a particular configuration, each one of the theoretical stretch curves presented in the next section is an average of 10 curves similar to those obtained with the 10 different random number sequences used in Figs 12 and 13.

RESULTS AND COMPARISON WITH EXPERIMENTS

We compare our theory with hydrodynamic stretch experiments by Chu's group (Perkins et al., 1995; Chu and Perkins, 1996, personal communication), and with electrophoretic stretch experiments by Smith and Bendich (1990) on fluorescently stained B-DNA. A B-DNA chain is characterized hydrodynamically by its contour length, L, the persistence length, P, and the hydrodynamic diameter, d. The persistence length of stained DNA is not accurately known. Fig. 14 shows hydrodynamic stretch curves of 21.8-μm-long DNA calculated assuming, from top to bottom, a persistence length of $P = 850$ Å, 675 Å, and 500 Å. The dependence of the curves on the persistence length is significant. The agreement of the middle curve with the experimental points is reasonable. From single chain experiments (Smith et al., 1992; Smith and Bendich, 1990) on stained DNA Smith (personal communication, 1996) has derived $P = 675$ Å, the value we adopt in this paper. It is somewhat larger than the 575 Å expected at equivalent ionic strength (10 mM) for double helical DNA (Baumann et al., 1997). The difference, if significant, may simply reflect a

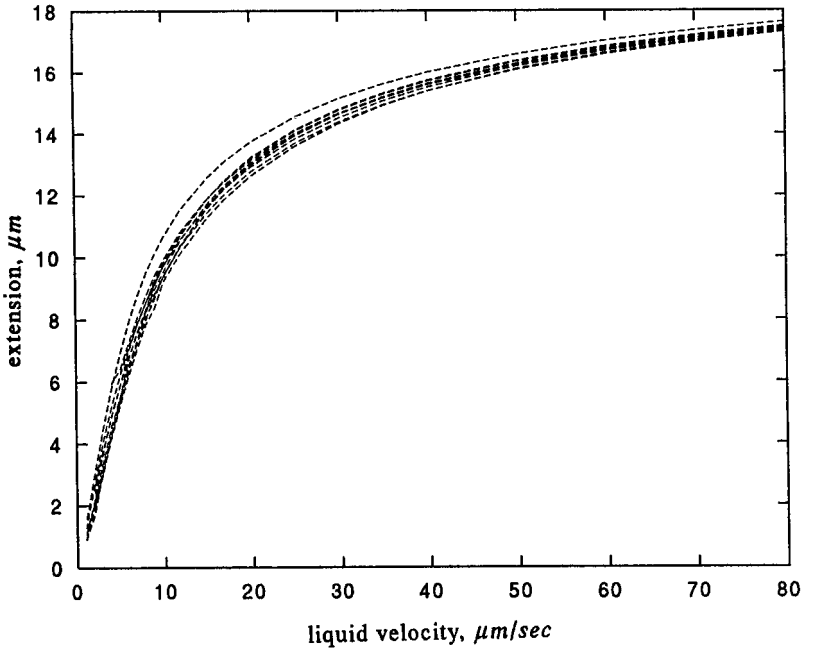

FIGURE 13 Extension-flow curves for the 10 random number sequences used for the conformations in Fig. 12.

stiffening effect on the chain of the intercalating fluorescent tag. Following Schellman and Stigter (1977) we take $d = 24$ Å for the kinetic diameter of B-DNA, consistent with diffusion and viscosity experiments. For the hydrodynamics we choose ellipsoidal segments with a long axis $2P = 1350$ Å and with the same volume as the cylindrical chain segments with diameter d, as suggested by Garcia de la Torre and Bloomfield (1977). This gives $c = d\sqrt{1.5}$ for the short axes of the ellipsoid in Eqs. 6 and 7. We find from Eqs. 6 and 7 that for such segments the radius of the equivalent Stokes sphere in Eq. 9 is $a_j = 111.9$ Å for parallel orientation and $a_j = 179.2$ Å for perpendicular orientation. In all hydrodynamic stretch computations we take $\eta = 0.95\ cP$, the value in the experimental work (Perkins et al., 1995). In the electrophoretic work we assume the water value at 25°C, $\eta = 0.89\ cP$.

Figs. 14 and 15 compare the theory with DNA experiments over the range of contour lengths for which experimental data are presently available, 21.8 μm to 151 μm. Over this large size range the differences between theory and experiment are quite small.

The Smith and Bendich (1990) electrophoretic stretch experiments were carried out in 0.045 M Tris base, 0.045 M boric acid, 0.001 M EDTA, and 0.5 μg/ml ethidium bromide. We estimate from later experiments by Smith et al. (1992) that in such a medium ethidium intercalation lengthens B-DNA by 31%. We assume that one ethidium increases the contour-length by 3.37 Å, the same as one basepair. Then, with one positive charge per ethidium, the stained DNA has a fixed linear charge density of $(2 - 0.31)/(3.37 \times 1.31) = -0.383\ e$/Å. We evaluate the ζ potential of the stained DNA with the nonlinear Poisson-Boltzmann equation (Stigter, 1975). We assume that the ionic medium is equivalent to 0.01 M $N(CH_3)_4Cl$, and that no counterions are inside the shear surface located 12 Å from the axis of the DNA cylinder. Then we find for the surface potential of such a cylinder $e\zeta/kT = -4.65$ or $\zeta = -0.1195$ V. Applying Eqs. 24 and 25, the electrophoretic mobility of stained DNA oriented parallel to the applied field is $\nu_\parallel/E \cos \theta_i = -7.96 \times 10^{-8} m^2 s^{-1} V^{-1}$ and, with $g_\perp = 0.484$ (Stigter, 1991), the mobility perpendicular to the applied field is $\nu_\perp/E \sin \theta_i = -2.57 \times 10^{-8} m^2 s^{-1} V^{-1}$.

In Fig. 16 the theory is compared with the experiments by Smith and Bendich (1990) on circular 66 kbp plasmids, immobilized by agarose fibers threaded through their centers. The agarose gel was cast between a microscope slide and a coverslip. The extension was measured of the stained DNA held at the surface of the gel in an electric field applied parallel to the coverslip. The authors state that "the high end of the distribution [of the points in Fig. 16] should represent the unobstructed molecules hooked at one end." Fig. 16 shows that the solid curve for the theory is near the upper boundary of the experimental points. This agreement between theory and experiment may be fortuitous because of 1) possible electroosmotic flow in the gelfree solution between gel and coverslip, 2) possible interaction of the two proximate chains of the circular DNA treated as a single chain in the theory, and 3) possible depression of intersegment hydrodynamic interaction in the DNA chains due to the proximity of gel and coverslip.

The dashed curve in Fig. 16 is the extension calculated with Eq. 27 for F_i, instead of Eq. 29; that is, without any hydrodynamic interaction between segments. The difference with the solid curve shows the large effect of this long-range interaction. It is likely that in DNA chains stretched during gel electrophoresis the long-range intersegment interactions are considerably weakened.

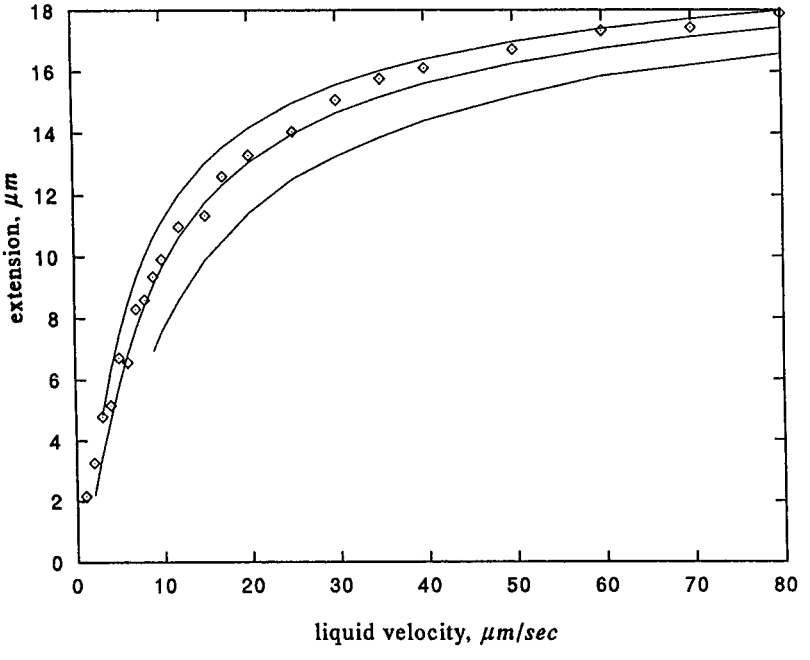

FIGURE 14 Extension-flow curves for 21.8-μm-long DNA calculated with different persistence lengths. From top to bottom: $P = 850$ Å, 675 Å, 500 Å. Points from experiments by Perkins et al. (1995; personal communication, 1996).

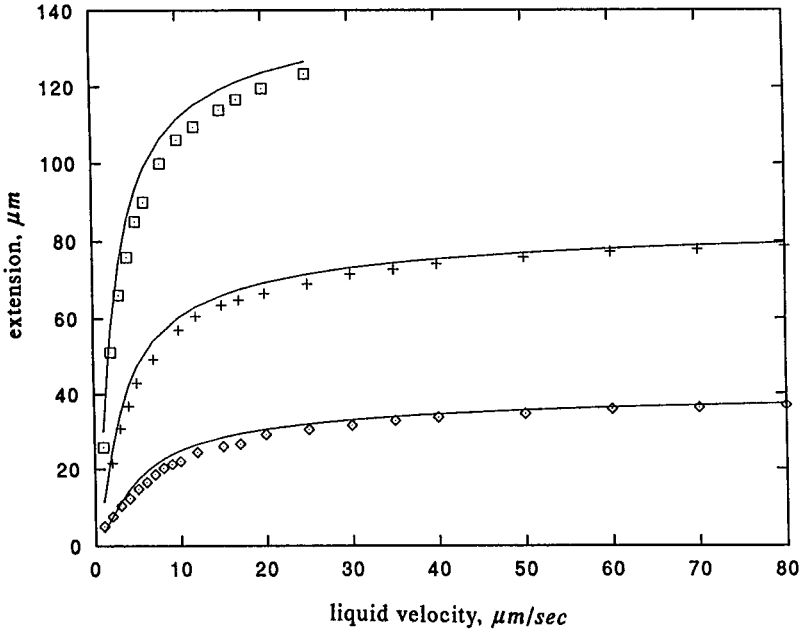

FIGURE 15 Extension-flow curves for DNA with different contour lengths. From top to bottom: L = 151.0 μm, 89.6 μm, 44.0 μm. Points from experiments by Perkins et al. (1995; personal communication, 1996).

It is possible to determine the total force on the DNA tethered to a bead fixed in a laser trap by measuring the deflection of the laser beam. To our knowledge such experiments have not been reported. Therefore, here we give only some sample curves. Fig. 17 shows the tethering force as a function of flow velocity as obtained from Eq. 14 for 21.8- and 44.0-μm-long stained DNA, lower and upper curves, respectively. The solid curves are for the case of full intersegment interaction, Eqs. 5, 8, and 10. In the dashed curves the intersegment interaction is omitted, i.e., $\Delta u_{ij} = 0$ in Eq. 8. It is found that this long-range hydrodynamic interaction reduces the force by ~60%. The results show also that the total friction force is approximately proportional to the contour length of the DNA and to the flow rate.

Fig. 18 gives force versus electric field curves for stained DNA with contour length 21.8 μm. As in Fig. 17, the solid curves are calculated with intersegment interactions (Eq. 29), the dashed curves are obtained without intersegment interactions, using Eq. 27. The three sets of curves are for three different ionic strengths, from top to bottom 0.01 M ($e\zeta/kT = -4.65$, $g_\perp = 0.484$), 0.03 M ($e\zeta/kT = -3.67$, $g_\perp = 0.551$), and 0.1 M ($e\zeta/kT = -2.67$, $g_\perp = 0.655$). The difference between the dashed and the solid curves shows that for the tethered DNA the electrophoretic force is re-

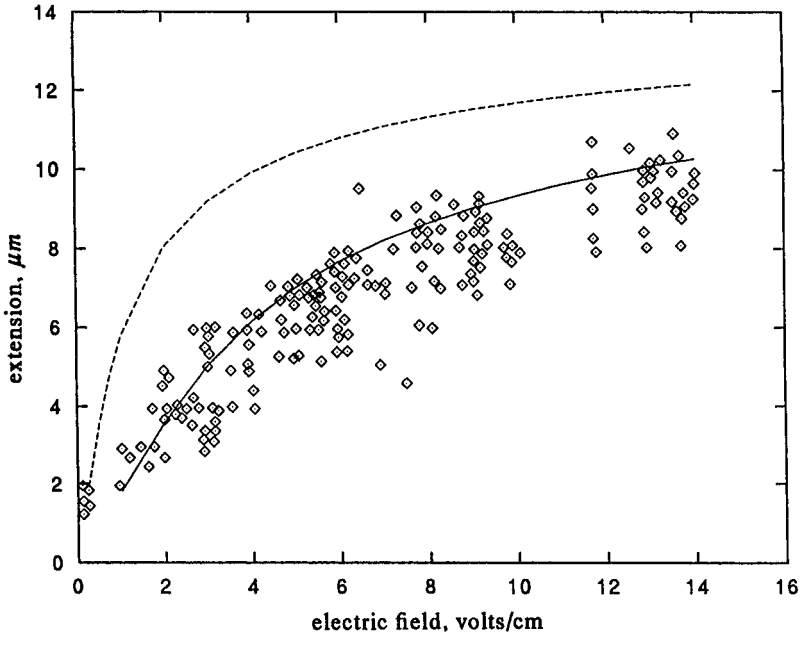

FIGURE 16 Extension-electric field curves for 14.7-μm-long DNA from full theory (*solid curve*) or without hydrodynamic interaction between segments (*dashed curve*). Points from Smith and Bendich (1990).

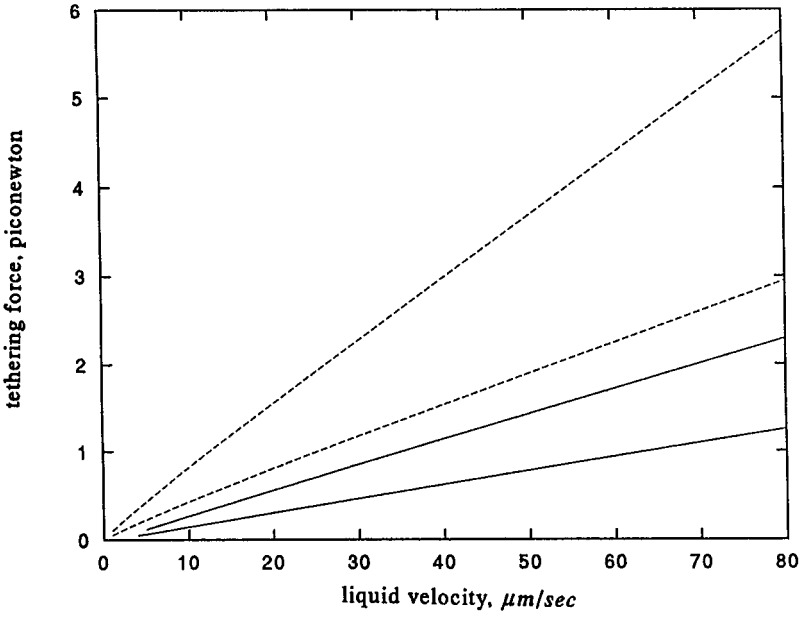

FIGURE 17 Tethering force-flow curves for DNA from full theory (*solid curves*) or without hydrodynamic interaction between segments (*dashed curves*). *Upper curves*: $L = 44.0$ μm. *Lower curves*: $L = 21.8$ μm.

duced to ~⅓ of its original value by the long-range hydrodynamic interactions. The influence of the ionic strength on the force is substantial. The deviation from linearity of the curves is somewhat greater than in Fig. 17, presumably because of a greater net effect of the chain conformation on the electrophoretic force.

CONCLUSIONS

We have treated the extension of polyelectrolytes such as B-DNA tethered at one end in a uniform liquid flow, or in an external electric field. We include long-range hydrodynamic interaction between ellipsoidal chain segments and electric field effects on the small ions. Predictions are in good agreement with hydrodynamic stretch experiments by Perkins et al. (1995, personal communication, 1996) and with electrophoretic stretch experiments by Smith and Bendich (1990) on fluorescently stained B-DNA. This shows that the polyelectrolyte models developed to interpret macroscopic experiments can be used for single molecule experiments.

We use the Marko-Siggia (1995) results for the force-extension relation, as in earlier treatments of electrophoretic stretch (Marko and Siggia, 1995) and hydrodynamic stretch (Marko and Siggia, 1995; Larson et al., 1997; Zimm, 1997, personal communication). The emphasis is on an accurate treatment of the tension in the chain, on the basis of structural information without adjustable parameters. To treat

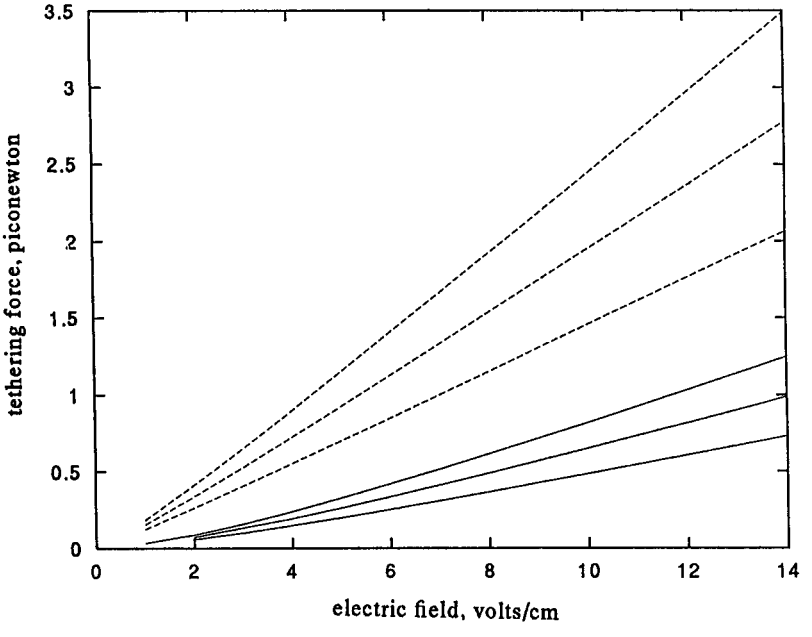

FIGURE 18 Tethering force-electric field curves for 21.8-μm-long DNA in different ionic strength solutions calculated from full theory (*solid curves*) or without hydrodynamic interaction between segments (*dashed curves*). Ionic strength from top to bottom: 0.01 M, 0.03 M, 0.1 M.

hydrodynamic and electrophoretic stretch on an equal footing, we use long ellipsoidal chain elements for hydrodynamic friction (Oberbeck, 1876) and long cylindrical chain elements for electrophoretic forces (Stigter, 1991). Unlike earlier models (Marko and Siggia, 1995; Larson et al., 1997), the present model describes chain orientational effects that lead to different force-extension curves for flow and electric fields. This shows that the "equivalence" proposal by Long et al. (1996a,b) is not valid, except for low extensions. The tethering force is found to be roughly proportional to the flow velocity or field strength, and to the contour length of the polyelectrolyte. The explicit treatment of long-range hydrodynamic interactions in our model is an advantage in applications to gel electrophoresis when such interactions may be partly or wholly damped by the surrounding gel.

The authors are indebted to Professor Steven Chu and Thomas T. Perkins for making hydrodynamic stretch data available. We thank Professor Bruno Zimm for stimulating discussions and for a preview of his work, and Steven Smith for helpful discussions and a critical reading of the paper.

This work was supported by National Science Foundation Grants MBC 9118482 and BIR 9318945, and National Institutes of Health Grant GM-32543.

REFERENCES

Baumann, C. G., S. B. Smith, V. A. Bloomfield, and C. Bustamante. 1997. Ionic effects on the elasticity of single DNA molecules. *PNAS.* 94: 6185–6190.

Bustamante, C., J. F. Marko, E. D. Siggia, and S. Smith. 1994. Entropic elasticity of λ-phage DNA. *Science.* 265:1599–1600.

Doi, M., and S. F. Edwards. 1986. The Theory of Polymer Dynamics. Cambridge University Press, New York, NY.

Flory, P. J. 1953. Principles of Polymer Chemistry. Cornell University Press, Ithaca, NY.

Garcia de la Torre, J., and V. Bloomfield. 1977. Hydrodynamic properties of macromolecular complexes. I. Translation. *Biopolymers.* 16: 1747–1763.

Happel, J., and H. Brenner. 1965. Low Reynolds Number Hydrodynamics. Prentice Hall, Englewood Cliffs, NJ.

Hermans, J. J. 1949. *In* Colloid Science, Vol. 2. H. R. Kruyt, editor, Elsevier, New York, 117–118.

Hill, T. L. 1960. Introduction to Statistical Thermodynamics. Addison-Wesley, Reading, MA.

Kirkwood, J. G., and J. Riseman. 1948. The intrinsic viscosities and diffusion constants of flexible macromolecules in solution. *J. Chem. Phys.* 16:565–573.

Kramers, H. A. 1946. The behavior of macromolecules in inhomogeneous flow. *J. Chem. Phys.* 14:415–423.

Landau, L. D., and E. M. Lifshitz. 1958. Statistical Physics. Pergamon, New York.

Landau, L. D., and E. M. Lifshitz. 1982. Fluid Mechanics. Pergamon, New York.

Larson, R. G., T. T. Perkins, D. E. Smith, and S. Chu. 1997. Hydrodynamics of a DNA molecule in a flow field. *Phys. Rev. E.* 55:1794–1797.

Long, D., J. Viovy, and A. Ajdari. 1996a. Simultaneous action of electric fields and nonelectric forces on a polyelectrolyte: motion and deformation. *Phys. Rev. Lett.* 76:3858–3861.

Long, D., J. Viovy, and A. Ajdari. 1996b. Stretching of DNA with electric fields revisited. *Biopolymers.* 39:755–759.

Marko, J. F., and E. D. Siggia. 1995. Stretching DNA. *Macromolecules.* 28:8759–8770.

Oberbeck, A. 1876. Ueber stationäre Flüssigkeitbewegungen mit Berücksichtigung der inneren Reibung. *Crelles J.* 81:62–80.

Perkins, T. T., D. E. Smith, R. G. Larson, and S. Chu. 1995. Stretching of a single tethered polymer in a uniform flow. *Science.* 268:83–87.

Schellman, J. A., and D. Stigter. 1977. Electrical double layer, zeta potential, and electrophoretic charge of double-stranded DNA. *Biopolymers.* 16:1415–1434.

Schurr, J. M., and S. B. Smith. 1990. Theory for the extension of a linear polyelectrolyte attached at one end in an electric field. *Biopolymers.* 29:1161–1165.

Smith, S. B., and A. J. Bendich. 1990. Electrophoretic charge density and persistence length of DNA as measured by fluorescence microscopy. *Biopolymers.* 29:1167–1173.

Smith, S. B., Y. Cui, and C. Bustamante. 1996. Overstretching B-DNA: the elastic response of individual double-stranded and single-stranded DNA molecules. *Science.* 271:795–798.

Smith, S. B., L. Finzi, and C. Bustamante. 1992. Direct mechanical measurements of the elasticity of single DNA molecules by using magnetic beads. *Science.* 258:1122–1126.

Stigter, D. 1975. The charged colloidal cylinder with a Gouy double layer. *J. Colloid Interface Sci.* 53:296–306.

Stigter, D. 1978a. Electrophoresis of highly charged colloidal cylinders in univalent salt solutions. 1. Mobility in transverse field. *J. Phys. Chem.* 82:1417–1423.

Stigter, D. 1978b. Electrophoresis of highly charged colloidal cylinders in univalent salt solutions. 2. Random orientation in external field and application to polyelectrolytes. *J. Phys. Chem.* 82:1424–1429.

Stigter, D. 1982. Primary charge effect on the sedimentation of long, colloidal rods. *J. Phys. Chem.* 86:3553–3558.

Stigter, D. 1991. Shielding effects of small ions in gel electrophoresis of DNA. *Biopolymers.* 31:169–176.

Vologodskii, A. 1994. DNA extension under the action of an external force. *Macromolecules.* 27:5623–5625.

Wang, M. D., H. Yin, R. Landick, J. Gelles, and S. M. Block. 1997. Stretching DNA with optical tweezers. *Biophys. J.* 72:1335–1346.

Yamakawa, H., and M. Fujii. 1973. Translational friction coefficient of wormlike chains. *Macromolecules.* 6:407–415.

Yamakawa, H., and M. Fujii. 1974. Intrinsic viscosity of wormlike chains. Determination of shift factor. *Macromolecules.* 7:128–135.